remote sensing

MDPI

Article

Mapping Crop Planting Quality in Sugarcane from UAV Imagery: A Pilot Study in Nicaragua

Inti Luna [1,*] and Agustín Lobo [2]

[1] Evolo Company, Reparto San Juan 142-A, Managua, Nicaragua
[2] Instituto de Ciencias de la Tierra "Jaume Almera" (CSIC), Lluis Solé Sabarís s/n, 08028 Barcelona, Spain; agustin.lobo@ictja.csic.es
* Correspondence: intiluna@gmail.com; Tel.: +505-8756-6013

Academic Editors: Clement Atzberger and Prasad S. Thenkabail
Received: 10 April 2016; Accepted: 7 June 2016; Published: 14 June 2016

Abstract: Sugarcane is an important economic resource for many tropical countries and optimizing plantations is a serious concern with economic and environmental benefits. One of the best ways to optimize the use of resources in those plantations is to minimize the occurrence of gaps. Typically, gaps open in the crop canopy because of damaged rhizomes, unsuccessful sprouting or death young stalks. In order to avoid severe yield decrease, farmers need to fill the gaps with new plants. Mapping gap density is therefore critical to evaluate crop planting quality and guide replanting. Current field practices of linear gap evaluation are very labor intensive and cannot be performed with sufficient intensity as to provide detailed spatial information for mapping, which makes replanting difficult to perform. Others have used sensors carried by land vehicles to detect gaps, but these are complex and require circulating over the entire area. We present a method based on processing digital mosaics of conventional images acquired from a small Unmanned Aerial Vehicle (UAV) that produced a map of gaps at 23.5 cm resolution in a study area of 8.7 ha with 92.9% overall accuracy. Linear Gap percentage estimated from this map for a grid with cells of 10 m × 10 m linearly correlates with photo-interpreted linear gap percentage with a coefficient of determination (R^2)= 0.9; a root mean square error (RMSE) = 5.04; and probability (p) << 0.01. Crop Planting Quality levels calculated from image-derived gaps agree with those calculated from a photo-interpreted version of currently used field methods (Spearman coefficient = 0.92). These results clearly demonstrate the effectiveness of processing mosaics of Unmanned Aerial System (UAS) images for mapping gap density and, together with previous studies using satellite and hand-held spectroradiometry, suggests the extension towards multi-spectral imagery to add insight on plant condition.

Keywords: UAV; sugarcane; gap; planting quality; precision agriculture; Nicaragua

1. Introduction

Sugar is an important ingredient in the human diet that is mainly produced from sugarcane (*Saccharum* spp. hybrid) in more than one-hundred countries within the latitude belt 37°N to 31°S [1]. Sugarcane is also being used for bio-ethanol production, power generation from cane residues [2], and other minor products such as bagasse, molasses and cane wax [3]. In 2014, sugarcane crops in the world were using 27.2 million hectares [4]. Sugarcane cultivation is widespread in Central America, covering 616,706 ha [4], and is a key component for the Nicaraguan economy, which had 71,347 ha used for sugarcane, producing an average of 88.8 tons per ha during the harvest of 2014–2015 [5], and 77.4% of the land devoted to sugarcane cultivation in Nicaragua is concentrated in the northwestern region of the country [6].

Global harvest of sugarcane had a nearly sixfold increase from 1950 to 2007 while harvested area increased 3.5 times according to data collected by the Food and Agriculture Organization of the

United Nations FAO [7]. To cope with the increasing demand for sugar and other sugarcane products, many companies and farmers are expanding sugarcane plantations to new areas, clearing forest and displacing more traditional crops in tropical areas with the consequent biodiversity loss [8–10]. Increasing yield and improving cropping efficiency are key points in a strategy for reducing agricultural expansion and environmental footprint [11]. Proof that more attention should be given to increase yield and efficiency is that Nicaragua decreased its average yield in 7.6%, and crop areas continued to expand during harvest 2015–2016 [12].

Sugarcane is a semi-perennial crop that tends to reach its maximum vegetative development during a grand growth stage of around 120 days to 270 days after planting in a 12-month cane [13]. Main sugarcane varieties found in Nicaragua are from the Canal Point Sugarcane Research Station, City, Florida, US and are CP722086, CP892143 and CP731543. In general, a crop of cane takes about 12–13 months to grow in Leon and Chinandega, provinces on the pacific coast of Chinandega. Most large sugarcane plantations in Nicaragua divide their crop areas into three management zones with different planting and harvesting times. Typical harvesting periods in a year are: (i) November to January; (ii) January to March; and (iii) March to April, before rainy season starts (commonly in May) and harvesting labor increases its cost related to wet terrain and increasing transportation time of cane to the mill. In general, a cropping cycle is comprised of one plant crop and 4–5 ratoon (regrowth) crops. When ripe, the cane is usually about 2–3 m tall.

The first growth stage of sugarcane production is called the germination and establishment phase [14]. This phase takes place at the beginning of the cycle (around 10–15 days after harvest depending on cane variety). Normally, there are areas in the plantation where stalks do not develop, either because rhizomes were damaged during previous agronomic activities such as harvest (machines passing over croplines) due to unsuccessful sprouting, or because of death of young stalks caused by pests, diseases or inappropriate water distribution [15]. All of these causes result in the appearance of patches devoid of crop, commonly known as gaps. Farmers need to fill the gaps in the crop lines with new plants; otherwise, yield severely diminishes [16]. According to field data, gap percentage could be as high as 30% in certain plots in Nicaragua, although this figure is subject to large uncertainty because current gap assessment methods do not obtain sufficient, precise nor cost effective information.

An operational methodology for the field assessment of gap area by measuring gap length along segments of crop lines proposed by Stolf in Brazil [17] is being used nowadays with minor modifications. By collecting gap percentage at different plots, the manager can classify plantation zones according to crop planting quality and decide whether to replant one specific area or the whole plot. An important drawback of this method is that it requires a very intense field effort. Methods using sensors on land vehicles have been developed and tested [18,19] require circulating over the entire plantation, which is costly in time and fuel, and increases the risk of damaging the crop.

Agriculture has been an important field of application for Remote Sensing (RS) since the earliest days (*i.e.*, Neblette 1927 and 1928 in [20]), and the interest increased with the advent of civil satellite imagery. Agricultural applications have surpassed the initial goals of crop acreage and mapping to include crop health and yield assessment. According to Atzberger [21], there are five application domains of RS in agriculture: biomass and yield estimation, crop vigor and drought stress monitoring, assessment of crop phenological development, crop acreage and mapping, and mapping disturbance and other changes. Nowadays, precision agriculture has triggered an important effort by the Remote Sensing community to provide timely geo-referenced information on crop condition (density, vigor, phenological stage, water, nutritional status) with sufficient resolution. Crop scouting has been traditionally used to provide this information, but scouting is slow, time and labor intensive, often expensive, and the quality of its results is difficult to assess, hence the renewed interest in Remote Sensing. A wealth of research is being carried out on the use of sophisticated instruments aboard satellites and airplanes to relate critical plant properties to sensor measurements (*i.e.*, [22–24]). The challenge is achieving operational methods able to be applied within reasonable budgets, a goal that has to be met at on-farm level [20].

Abdel-Rahman and Ahmed [25] reviewed studies on RS applications to sugarcane cultivation. Most studies were based on satellite imagery and dealt with a range of applications such as mapping sugarcane over large areas, varietal identification, detection of stress (caused by diseases, pests and nutrient and water deficiencies) and yield prediction. The authors reported many successful studies, although this was not always the case, in particular when many confounding factors were present. It is worthwhile to note that studies conducted with hand-held spectrometers (*i.e.*, [26,27]) achieved good results. Research carried out with spectrometers indicates that it is possible to retrieve nitrogen content [28] and the nitrogen/silicon ratio [23], which are critical data for fertilizing plans and yield forecasting. Schmidt *et al.* [29] conducted a study using a Digital Multi-Spectral Video camera mounted on a microlite, which is a small fixed-wing mono motor plane, over sugarcane fields. Results were good for the discrimination of age groups, crop moisture stress and variety identification, but not for yield prediction and fertilizer application, although the authors reported "numerous teething problems in data acquisition and camera equipment setup".

The use of mini Unmanned Aerial Vehicles (UAV) or Remote Piloted Aircraft Systems (RPAS), a.k.a. "drones", is revolutionizing Remote Sensing and is increasingly applied to diagnose agricultural fields [30–33]. This technology has reached operational reliability and offers the possibility to map and monitor small areas, a task that would be very expensive by an aircraft, especially when the farm to monitor is not close to an airport. Therefore, RS from UAVs can be, in principle, a solution to incorporate RS at on-farm level. Nevertheless, it also must be considered that sensors aboard mini UAVs must be miniaturized versions of those traditionally used from satellites and airplanes because size and weight constraints, with the resulting lower quality, which has to be added to the inherent instability of a small platform. Therefore, it is important to test whether a particular agricultural application can be satisfactorily achieved by using instruments aboard a mini UAV.

Considering the critical importance of a correct assessment and the mapping of gap percent for optimizing sugarcane cultivation, the goal of this study was to assess, within the economic constraints of a developing country, the appropriateness of conventional digital imagery acquired from a mini-UAV for this purpose, using a photo-interpreted version of Stolf's methodology as a reference.

2. Methods

2.1. Study Site and Aerial Campaign

The UAV imagery was acquired over a plot of sugarcane named El Gobierno (12.448192°N, 87.053016°W and 19 m above sea level). The El Gobierno plot belongs to a 12,000 ha plantation located in the NW of Nicaragua, Central America (Figure 1) in the departments of Leon and Chinandega. The region has tropical savanna climate classified as "Aw" in the Köppen and Geiger system. Daily mean temperature ranges from 27.0 to 27.4 °C and rainfall from 1592 to 1979 mm. [34]. Most common soil orders in the area are inceptisols, entisols and vertisols, which are of volcanic origin [35].

The flight mission was planned with Lentsika software (2010 version from CEPED co, Torino, Italy), which transformed the overlaps and pixel size requirements into flight commands and parameter information for the autopilot. However, Lentsika software does not take into account specific camera features that are required to accomplish an accurate pixel size estimation; thus, further calculations had to be made and the Lentsika information was used only as a rough estimation.

A 16 min flight at 190 m above ground level with an overlap of 90% and a sidelap of 50% was carried out with the UAV to cover 24 hectares of the El Gobierno plot, registering 134 images with an average pixel resolution of 4.7 cm (Figure 2).

Figure 1. Location map of study area.

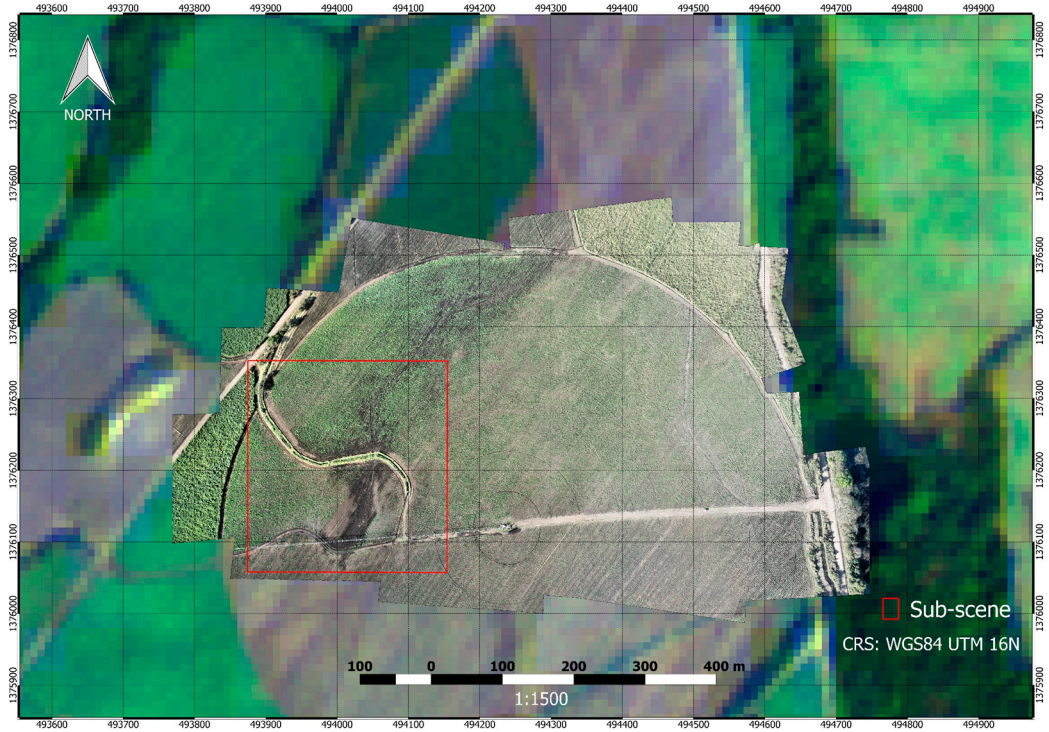

Figure 2. Mosaic of the 134 images acquired from the Unmanned Aerial Vehicle (UAV) over El Gobierno Plot, indicating the sub-scene processed in this study. Sentinel-2 red-green-blue (RGB) Image composition used as background.

2.2. UAV System

A Cropcam UAV with HORIZON ground control software (Micropilot Co., Stony Mountain, MB, Canada) was used for aerial image acquisition. The Cropcam weighs 3 kg, has a wingspan of 1.8 m and a maximum endurance of 45 min. In practice, due to payload weight, wind speed and

airframe modifications for a more stable flight and safe landing, endurance is reduced to 20 min at an average speed of 60 km/h. Our system includes a military grade autopilot unit (MP2028), which is a electromechanical system used to guide the plane without human assistance, in a radio controlled glider airframe. The autopilot guides the plane using GPS technology and differences in air pressure with a pitot tube in order to improve the speed control, flight performance and stability. The system has telemetry capacities, and transmits its position (x, y, z) to a computer using a radio modem, allowing the user to control the plane either via the radio control transmitter or via the computer. The autopilot supports multiple features and is programmable to fly a route and trigger a camera or other payload at specific locations.

The UAV was equipped with a conventional consumer grade still camera, a Canon SD780is with 5.9 mm focal length and a 1/2.3" CCD sensor (6.17 mm × 4.55 mm) of 12.1 mega pixels, that was mounted under the wing (Canon Inc., Tokyo, Japan).

2.3. Image Mosaicking and Geo-Referencing

A Mosaic with pixel resolution of 4.7 cm was produced by stitching the 134 images through PTGUI software, version 8.3.10 (New House Internet Services BV, Rotterdam, The Netherlands), and geo-referenced using the Georeferencer Tool plugin of Quantum Geograpic Information System (QGIS) software, version 1.7.4 [36] with a first-degree polynomial transformation. A high accuracy GPS for ground references was not available; therefore, pairs of ground control points were identified on the mosaic and Google Earth imagery that was used as a reference. The simple first-degree polynomial transformation could be used because the terrain was flat, the area small (24 ha) and few pairs of ground control points could be reliably identified. The resultant mosaic had a geometric error of 2.04 m estimated by identifying additional pairs of corresponding sites on the mosaic and Google Earth imagery. Reasons for this geometric error are given in discussion.

2.4. Stolf Method

Stolf [17] developed a methodology for assessing crop planting quality in sugarcane plantations based on gap evaluation, in which the lengths of gap segments are measured and added up along crop lines in the field. For practical reasons, gap segments are defined as those segments with no sugarcane plants or decayed sugarcane plants longer than 0.5 m. The method is applied by deploying a measuring tape on the ground and using a 0.5 m stick as the reference of minimum gap length. The length of so-defined gap segments is accumulated and the percentage of gap in a given distance is reported. Planting quality levels are defined based on gap percentage intervals as reproduced in Table 1.

Table 1. Thresholds of Gap percentage defining Planting Quality Levels according to Stolf, with permission from [17].

Gap Percentage	Planting Quality	Observations
0–10	Excellent	Exceptional germination conditions
10–20	Normal	Most common type observed
20–35	Subnormal	Possibility of renewal may be considered
35–50	Bad	Renewal should be considered
>50	Very bad	Renewal/Replanting

Obviously, not all crop lines can be measured at their entire length, as this would imply measuring (and walking) 6.5 km along crop lines for just a 1 ha plot. Aware of this, Stolf proposed measuring 4–5 random samples of 20–25 m for a 7 ha plot. Actually, current practices in El Gobierno are more intense: 1 random sample of 30 m is measured for each 0.7 ha plot (locally known as "manzana").

2.5. Processing

For this pilot study, we selected a sub-scene of 6272 lines × 5941 columns (8.2 ha) in the SW corner of the mosaic (Figure 3) and calculated a coarsened version with 23.5 cm resolution (1254 lines × 1188 columns) that was used for processing, keeping the higher-resolution version (4.7 cm per pixel) for photo-interpretation. As we detail in the following sub-sections, the processing method had two parts. First, we applied a supervised classification to create a binary image coded as "sugarcane" and "gap", where "gap" included bare soil and decayed plant material. Second, we estimated Gap percentage for a grid of 10 m × 10 m cells, and Crop Planting Quality Level following Stolf's standard thresholds (Table 1). This second step involved estimating Linear Gap percentage (gap estimates along lines) from the Gap percent based on the classification (thus a 2D estimate). Both processing steps required reference information that we produced through photo-interpretation of the 4.7 cm resolution mosaic.

Figure 3. Sub-scene of 6272 lines × 5941 columns (8.2 ha) in the SW corner of the mosaic reproduced in Figure 2.

All statistical processing and graphics were performed in R [37], with packages rgdal [38], raster [39], rgeos [40], MASS [41], ggplot2 [42] and plyr [43]. Display and exploration of imagery and spatial data sets was done in QGIS [36].

2.5.1. Reference Information

Actual field information was not available for this study, so we created two data sets of reference information (acting as "ground truth") through interactive photo-interpretation of the image at 4.7 cm resolution, in which plants could be distinguished. For the classification, we generated training and validation sets of point sites for which we determined whether the corresponding cover was sugarcane or gap. We defined a regular grid of 31 × 28 (768) cells of 10 m of side and selected a random subset of 25 cells. In order to create a training set of site observations for the supervised classification, we selected a random set of 300 point sites within the selected cells. These 300 points

were complemented by a set of 10 point sites randomly distributed over an area almost totally devoid of sugarcane and with notoriously darker soil. Photo-interpretation diagnosed each point site as "fresh sugarcane", "regular soil or withered sugarcane" or "dark soil". We discarded one point site because of dubious interpretation.

For the estimation of Linear Gap percentage, we digitized crop lines and gap lines in the random subset of 25 grid cells. This procedure actually mimics Stolf's method as performed in the field (see Section 2.4), although with much higher sampling intensity. We wrote an R script to import the shape files and calculated total row length, total gap length, Linear Gap Percentage and Crop Planting Quality Levels for each random cell.

In order to define the potential crop area, we digitized polygons of constant width (0.8 m) with axes coincident with those of the crop rows. We used these polygons to define the crop mask. We also digitized a mask of roads that included a small and narrow area (0.1 ha) between the limit of the road and the NW edge of the area of study to define areas not to be included in the surface calculations.

2.5.2. Classification

We retrieved the red (R), green (G) and blue (B) values corresponding to the 309 point sites from the image and generated a training data set with the red-green-blue bands (RGB) values as variables, and the diagnosed classes as grouping factors for running a Linear Discriminant Analysis (LDA [44]). LDA produced the transformation matrix for the canonical components and a cross-validated classification of the point sites. Cross-validation is a built-in method in the LDA function in R that consists of iteratively calculating the LDA excluding one element from the data set and predicting the class of the excluded element. This way, all elements were classified by a model that excluded the element for the fit. LDA output was used to display the point sites data on the canonical space, to build the confusion matrix and to calculate overall producer and user accuracies [45]. Finally, we used the fitted LDA model to predict the class of all pixels in the image, resulting in the "Classified Raster Layer".

2.5.3. Linear Gap Percentage and Crop Planting Quality Maps

We calculated "Gap Percentage" for each grid cell as the percentage of gap pixels in the corresponding areas of the Classified Raster Layer and within the area defined by the crop mask, excluding the area defined by the roads mask.

For the random sub-sample of 25 grid cells for which we had previously estimated "Linear Gap Percentage" by digitizing on the 4.7 cm resolution image (see Section 2.5.1):

(i) We compared boxplots of Gap and Linear Gap Percentage by "Crop Planting Quality Levels", to visually explore the appropriateness of the image-derived information to define "Crop Planting Quality Levels".

(ii) We fitted a linear regression model of "Linear Gap percentage" *vs.* "Gap percentage".

We applied the regression coefficients to calculate predicted "Linear Gap percentage" values to all grid cells and, from them, predicted "Crop Quality levels" by applying Stolf's standard thresholds (Table 1).

The accuracy of the regression model was assessed by its coefficient of determination (R^2) and root mean square error (RMSE), while the accuracy of predicted and the observed "Crop Planting Quality levels" was assessed by cross validation. To this end, we wrote an R script in which the regression is calculated with all data (from the subset of grid cells) but one, and the threshold applied to determine the predicted "Crop Planting Quality Level" of the excluded element. The script iterates in a manner that each element is excluded from the calculation of the regression model used to determine its predicted "Crop Planting Quality Level". These observed and predicted values were collected in a confusion matrix, thus allowing for an independent estimate of the accuracy, which was measured by the Spearman correlation coefficient (as corresponds to interval variables).

3. Results

We present our results organized in two parts. First, we present the results of the supervised classification (LDA) that creates a binary image of "sugarcane" and "gap". Second, we present the results of Gap percentage for a grid of 10 m × 10 m cells that is derived from the classification, including the relationship between linear (interactive) and classification-derived Gap percentages, and the final map of Crop Planting Quality Level (based on the grid of Gap percentage and Stolf's standard thresholds).

3.1. Classification

Figure 4 displays the distribution of point sites data on the canonical space and Table 2 presents the confusion matrix of the classification using cross-validation. Note that no discrimination can be achieved between classes "regular soil or withered sugarcane" and "dark soil" in the training set. Considering classifying soil types was not our goal, we reclassified by merging both classes into a "gap" class in both the confusion matrix and the classified image, thus defining "gap" as "no fresh sugarcane". The overall accuracy of this two-class confusion matrix (Table 3) was 97%, with 96.2% producer's accuracy and 97.6% user's accuracy.

While there is no omission error for gaps (that is, all sites that were photo-interpreted as gap were classified as gap), there is a commission error (some sites photo-interpreted as sugarcane were classified as gap), which implies that gap surface is overestimated by 4.9%.

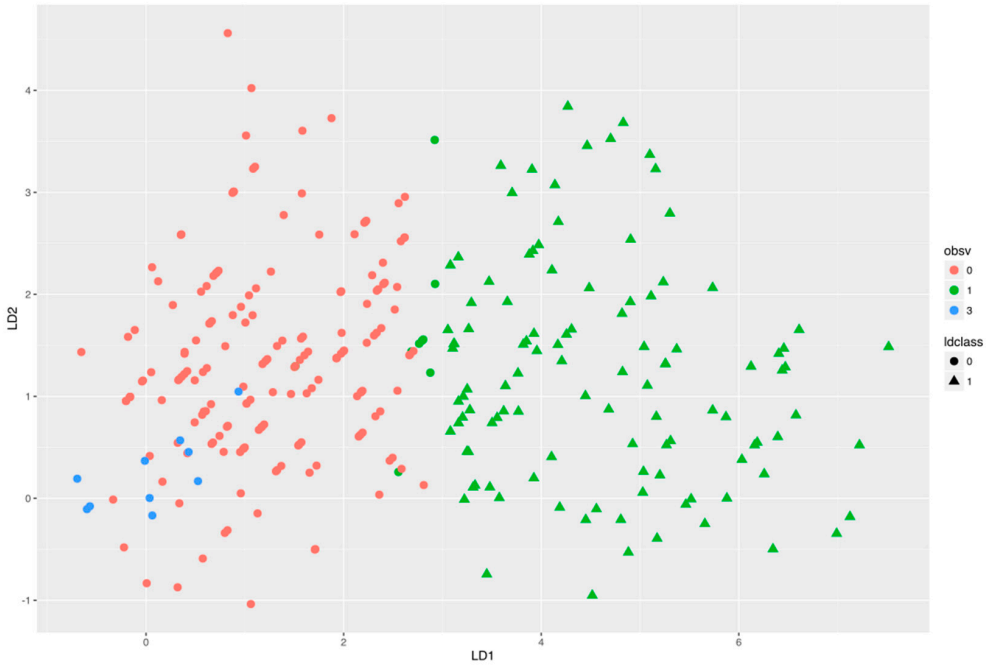

Figure 4. Scatterplot of the point sites data on the canonical plane. Colors refer to the diagnostics by photo-interpretation, shapes correspond to the classification. **Red**, regular soil or withered sugarcane; **blue**, dark soil; **green**, fresh sugarcane. Dots, soil or withered sugarcane (gaps); triangles, fresh sugarcane.

A confusion matrix generated from the photo-interpretation of a new, non-stratified set of 85 random sites (Table 3, values in parenthesis) resulted in lower accuracy values: 92.9% overall, 85.7 producer's and 95.7% user's accuracy. Again, no omission error but, proportionally, more sites were classified as gap while they were photo-interpreted as sugarcane than in the case of the cross-validation.

Table 2. Confusion matrix of the image classification (cross-validation).

		Image Classification		
		Regular Soil or Withered Sugarcane	**Fresh Sugarcane**	**Dark Soil**
Photo-interpretation	Regular soil or withered sugarcane	172	0	0
	Fresh Sugarcane	9	109	0
	Dark soil	10	0	0

Table 3. Confusion matrix after reclassification. Values calculated by cross-validation and for a set of 85 non-stratified random sites (in parentheses).

		Image Classification	
		Gap	**Sugarcane**
Photo-interpretation	Gap	182 (64)	0 (0)
	Sugarcane	9 (6)	109 (15)

In some cases, the misclassifications correspond to sites at the edge of sugarcane and background, which were photo-interpreted as sugarcane in the 4.7 cm resolution image but had a mixed color in the 23.5 cm resolution image and were thus classified as gaps. A second source of error was due to the fact that, for some parts of the image in which sugarcane appeared with a saturated, whitish color, the photo-interpreter could take into account additional information such as shape and lushness to decide that the given site was actually on sugarcane, while the classification, restricted to consider color values only, was indicating gap.

Figure 5 displays the vectorized version of the "Classified Raster Layer" overlaid to a zoomed portion of the full resolution image. The squares represent two of the 25 randomly distributed 10 m × 10 m cells used for the interactive measure of linear gap percentage.

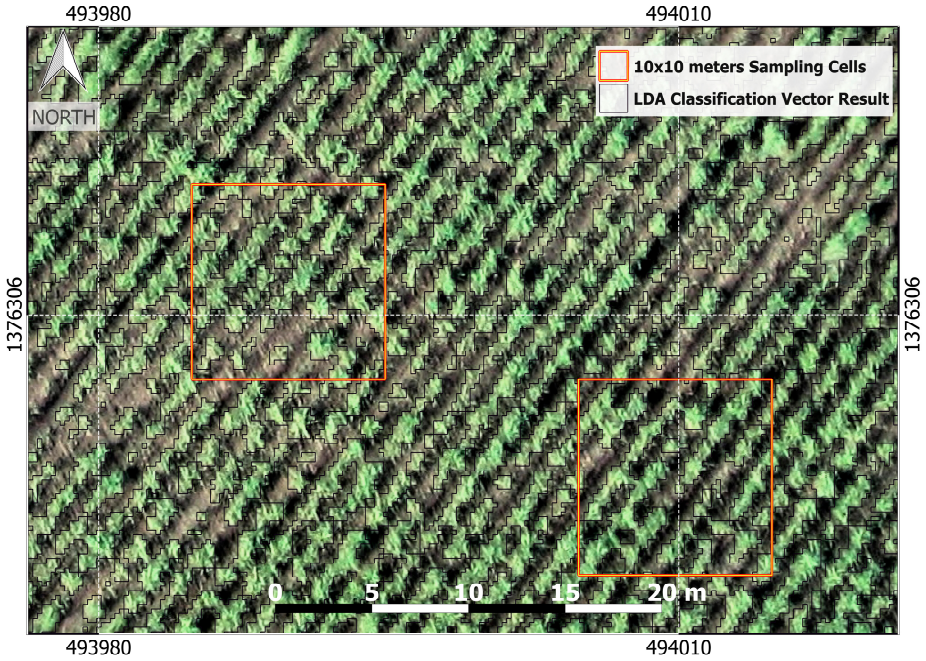

Figure 5. Details of the boundaries of the classification overlaid on the image.

3.2. Classification and Crop Planting Quality Levels

Figure 5 shows 2 of the 25 randomly distributed 10 m × 10 m cells used for the interactive measure of linear gap percentage. The scatterplot of Gap Percentages derived from the interactive digitizing *vs.* those derived from the image classification (Figure 6) displays the overall linear relationship between both variables. Gap percentages derived from the imagery are systematically higher than those derived from the interactive digitizing, which is explained by the fact that the interactive digitizing is based on a line following the axis of the crop while for the image derived values we used a rectangular mask that systematically includes some non-crop area. Nevertheless, the linear relationship is very strong, with an R^2 value of 0.9 (Table 4), which let us estimate Linear Gap Percentage from the image-derived values to apply Stolf's thresholds and calculate Crop Quality Levels using Table 1. The error shown by the scatter of the points in Figure 6 (RMSE of 5.04) was caused by the small misclassification rate mentioned in previous section, although some inconsistency in the photo-interpretation can never be ruled out.

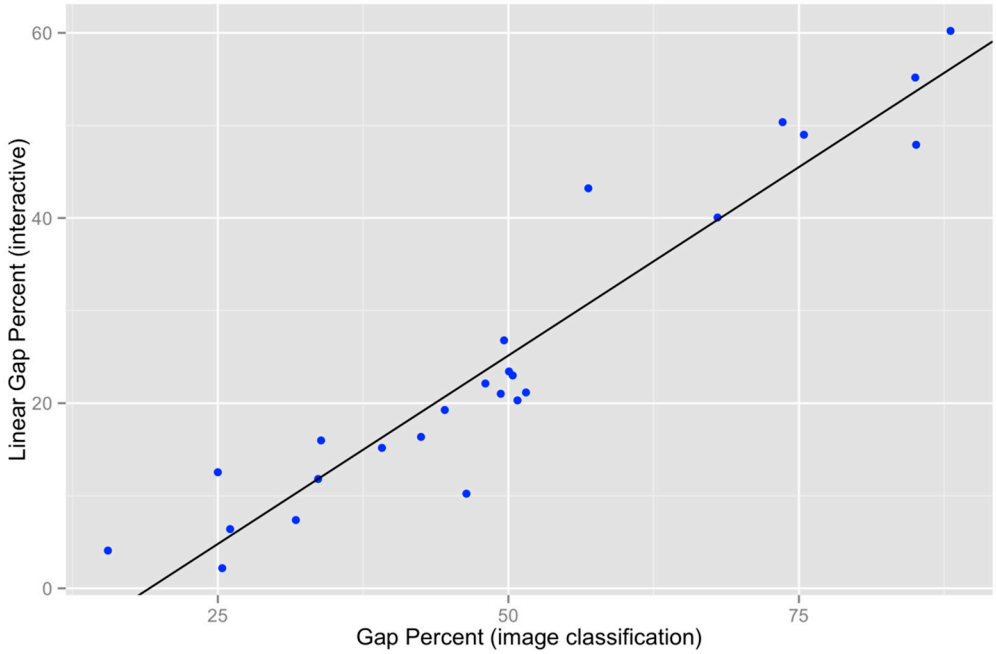

Figure 6. Scatterplot and linear fit of gap percentages derived from the interactive segments *vs.* those derived from the image classification for the subset of 10 m × 10 m grid cells. Regression line is $y = -15.56 + 0.81x$ ($R^2 = 0.91$, $p << 0.1$).

Table 4. Diagnostics of the linear model (Ordinary Least Squares fit) of gap percentages derived from the interactive segments (y) *vs.* those derived from the image classification (x) for the subset of 10 m × 10 m grid cells.

Statistic	Value	Standard Error	p
Intercept	−15.600	2.876	1.70×10^{-50}
Slope	0.814	0.054	1.85×10^{-13}
RSE	5.254	5.254	
R^2	0.909		
F	229.500 (23 d.o.f)		1.85×10^{-13}

Comparison of box-plots of Gap Percentages by Crop Planting Quality Levels (Figure 7) indicates that Gap Percentage derived from the image classification can be used to define Crop Planting Quality Levels consistently with levels defined from Linear Gap Percentage. This is confirmed by the confusion

matrix derived from the cross-validation of the predicted Crop Quality levels (Table 5), with a highly significant Spearman correlation of 0.92.

Figure 8 represents the map of Crop Planting Quality, in which levels are the predicted Crop Planting Quality Levels. According to this map, 55.4% of the area (=4.43 ha) is below the Normal level and requires some intervention. The map allows for estimate costs and action plans. Zooming into the 10 m × 10 m cells on the co-registered full-resolution image helps make decisions on the details of the actions.

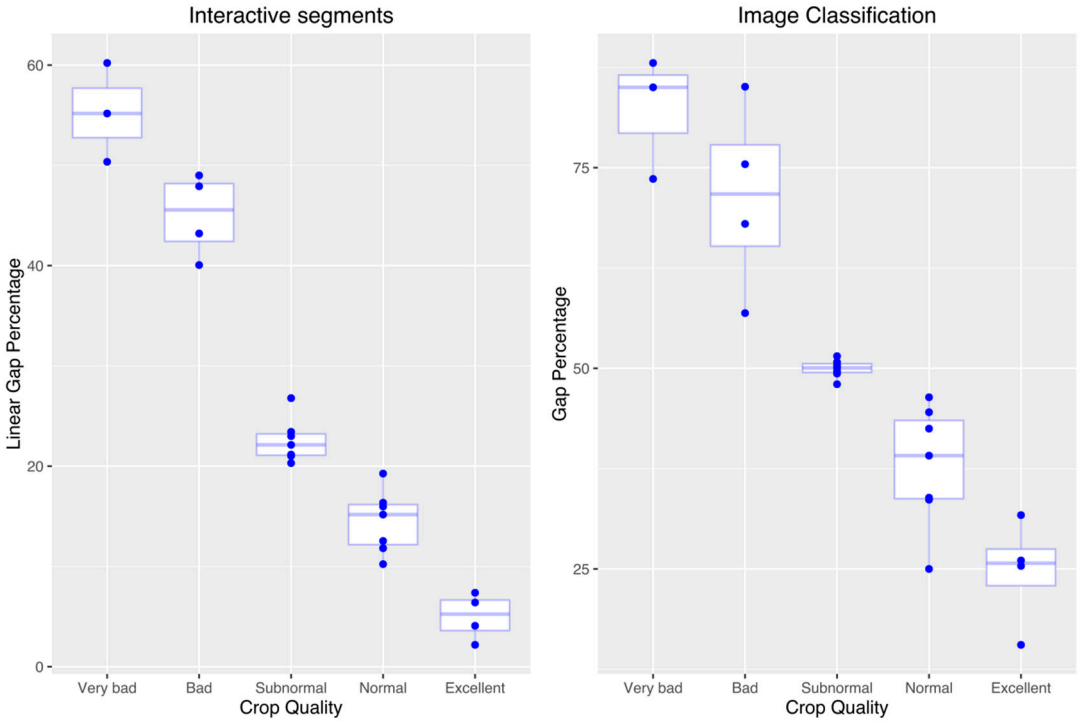

Figure 7. Boxplots of Gap Percentage by Crop Planting Quality Levels for the reference subset of 10 m × 10 m grid cells. (**left**) values from interactive segments; (**right**) values derived from image classification. Points indicate values for actual cells.

Table 5. Confusion matrix of the Crop Quality levels.

		Based on Gap Percentage (Image Classification)				
		Very Bad	**Bad**	**Sub-Normal**	**Normal**	**Excellent**
Based on Linear Gap Percentage (interactive)	Very Bad	2	1	0	0	0
	Bad	1	2	1	0	0
	Sub-Normal	0	0	7	0	0
	Normal	0	0	2	4	1
	Excellent	0	0	0	1	3

In summary:

- Classification by means of LDA results on a binary map of "sugarcane" and "gap" with an overall accuracy from 97% (estimated by cross-validation) to 92% (estimated by independent sub-sample);
- For grid cells of 10 m × 10 m, interactive Linear Gap percentage is linearly related to Gap percentage based on the classification (R^2 = 0.91, $p << 0.1$), which let us apply Stolf's standard thresholds to label Gap percentage as Crop Planting Quality Levels;

- The map of Crop Planting Quality is calculated from a 10 m × 10 m grid of Gap percentage derived from the classification. Crop Planting Quality from this grid agrees with Crop Planting Quality based on Interactive Linear Gap percentage (Spearman correlation 0.92).

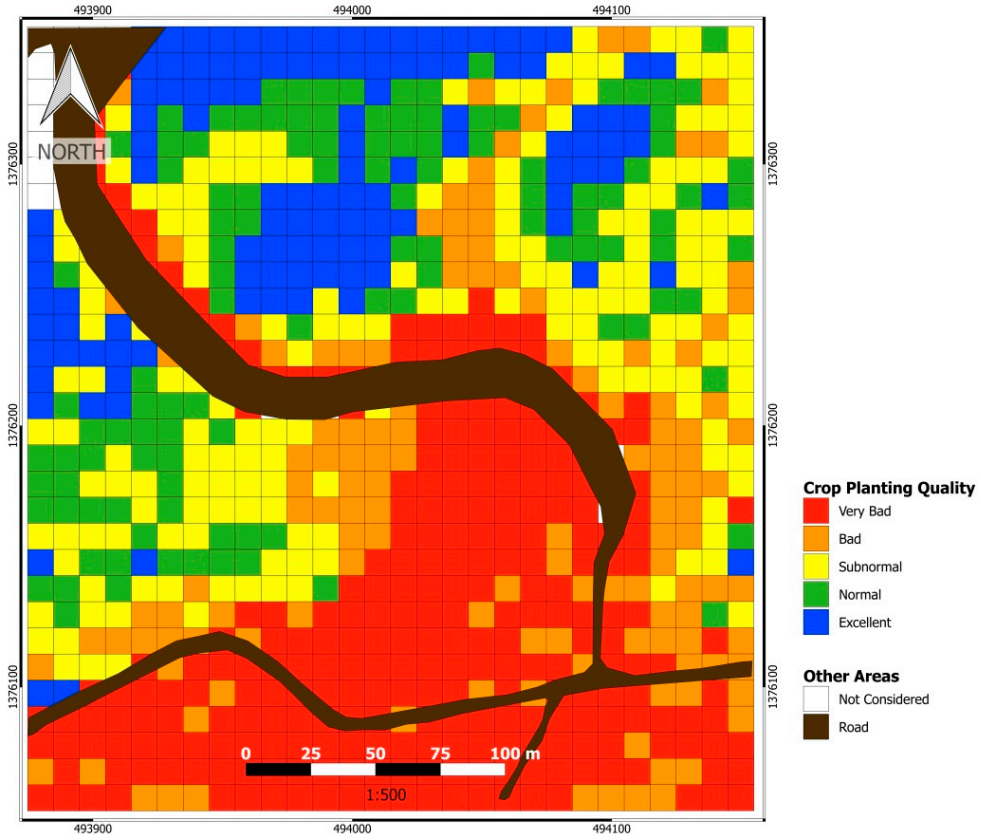

Figure 8. Map of Crop Planting Quality. Predicted Stolf Quality Levels derived from the UAV image.

4. Discussion

Our methodology is operational and outperforms current field methods, as the classification error is small and clearly compensated by the superior spatial intensity of an image-based method: current practices of field gap evaluation in El Gobierno (one segment of 30 m evaluated every 0.7 ha) would have implied evaluating 11 segments of 30 m, a length approximately equivalent to that of all crop lines within five plots of 10 m × 10 m, that is only about 0.45% of the total crop lines length. While this sampling intensity, which requires a very significant human effort, might provide some insight for monitoring overall crop planting quality, it is clearly insufficient to map gap percentage and derived crop planting quality, which makes re-planting activities very difficult to guide. Instead, our method uniformly maps Crop Planting Quality for the whole area by units of 10 m × 10 m.

In practice, for applying this methodology on a regular basis to a given plantation, Stolf's thresholds for Crop Planting Quality Levels would be calculated in terms of the classification-based gap percentage at the beginning of the study: the regression model relating linear (interactive) and classification-derived Gap percentages would be fitted once and would hold as long as the geometric arrangement of the plantation (and thus the fit of the rectangular mask to the crop rows) remain the same.

According to our evaluation, there is a very good agreement between our estimate of Crop Planting Quality and the one resulting from Stolf's method. The observed small discrepancy is due to classification error and to the differences in Gap percentage estimates between the linear (interactive) and the classification-based methods. Future improvements to the method should thus concern these

two aspects, with the addition of improving geometric accuracy. We briefly review these possible improvements in the rest of the Discussion and point out possible future related studies.

Besides the obvious improvement of using a better camera, improved image processing methods could reduce classification error further. Object-based recognition [46,47] could improve identifying sugarcane plants [48], and more sophisticated classification methods (notably Support Vector Machines [49,50]) will probably outperform LDA. It can be argued that requiring a training set of diagnosed sites could be seen as a drawback. While testing completely unsupervised methods is certainly of interest, generating a training set is not a very time-consuming task and the detailed inspection of the imagery is always interesting and worthwhile. The classification approach that is crucial in this methodology assumes that color is uniformly registered across the mosaic, which implies that care must be taken at image acquisition and mosaicking. While methods such as Contrast Limited Adaptive Histogram Equalization (CLAHE [51]) can be used in those cases in which the mosaic is not uniform, angular effects deserve more careful consideration in future studies [52].

Part of the dispersion of the regression model relating linear (interactive) and classification-derived Gap percentages is caused by the rectangular masks of the crop rows not fitting the actual irregular limits of the rows equally everywhere, as mentioned in Section 3.2. Image segmentation could be used to delineate crop rows [53] and produce an image-derived irregular mask fitting the actual crop instead of the digitized regular rectangles. Image segmentation has been applied to Unmanned Aerial System (UAS)imagery with similar purposes in orchards and vineyards (*i.e.*, [54,55]) In our case, the consistent generation of an adaptive mask would greatly increase the stability of the relationship between the linear (interactive) and the classification-based estimates of Gap percentage.

The elementary mosaicking and georeferencing methods that we have applied in this study are acceptable for very flat surfaces and yet have resulted in a large geometric error compared to pixel resolution. This error can be tolerated in this application because the final Crop Planting Quality product is a 10 m $\times$ 10 m grid, but would be an obvious problem for final products demanding finer resolution. More sophisticated mosaicking methods performing ortho-rectification are required in general for UAS imagery. Several commercial alternatives exist that use structure from Motion (SfM [56,57]) based software that apply automatic tie point generation, bundle block adjustment technology and efficiently generate ortho-rectified mosaics and digital surface models (also known as crop surface models, CSMs) with homogeneous radiometric responses. However, these types of products require ground control points (GCP) with high geometric accuracy, which is not easy for areas without unclassified high-resolution official orthophotomaps as in this case. Deploying markers on the ground and reading their coordinates with sub-metric (or even centimetric) accuracy is a very effective solution. Unfortunately, sub-metric or centimetric GPS equipment was not available for this study, but it is clearly a very needed piece of equipment for future campaigns, and acquisition should be facilitated by the current trend towards low-cost real time kinematics GPS (orRTK GPS) systems. Nevertheless, it must be noted that, while deploying ground markers on small areas such as the one of the sub-scene processed in this study (8.2 ha) is feasible, deployment of markers on larger areas such as the one of the entire mosaic (24 ha) will require a significant effort. This situation is pushing towards alternatives such as using RTK GPS during flight to get highly accurate camera locations data, thus avoiding the need of setting physical ground reference at the site while still getting high accuracy in final mosaic products [58].

Extending the method presented in this study to large plantations would have a considerable interest, making relevant the fact that Remote Sensing from UAVs should not be considered outside the framework of Remote Sensing from other vehicles. Large plantations will require optimizing pixel size to cover a large extent while keeping computing requirements within feasible limits on one hand, and sufficient gap detection on the other. Such an optimization implies a sensitivity analysis of gap detection to pixel length for each considered instrument (*i.e.*, [59–61]), a task for which the integration of UAV Remote Sensing from a range of heights, and satellite (*i.e.*, Sentinel-2) imagery would be most useful.

We have used Stolf's method in this study to demonstrate that image-derived gap percentage can map Crop Planting Quality levels as an effective and spatially intense alternative to field-estimated linear gap percentage because Stolf's method is currently the most common method. In addition, gaps are readily assessed by photo-interpretation of very high-resolution imagery because of their high contrast to fresh sugarcane. Nevertheless, estimating Crop Planting Quality based on gap percentage is not necessarily the only or the best method. It might very well be the case that our estimate of gap percentage could be better related to a more formal measure of crop quality such as green biomass rather than linear gap percent. In other words, alternative measures of crop planting quality at sampling sites in the field could be both more relevant agronomically and better related to image-derived information. Crop surface models, which would require high accuracy GCP and stereo images, should be investigated in sugarcane as it has provided useful data to study biomass in rice [62] and estimate yield in corn in conjunction with spectral data [63]. Furthermore, as multi-spectral imagery can provide information beyond gap percentage, for example on plant condition (see Introduction section), using a multi-spectral camera with bands going into the near-infrared region of the electromagnetic spectrum would represent an important improvement. It is relevant to note, though, that addressing the issue of remote sensing of plant condition goes well beyond simply using a better sensor, but involves ground sampling procedures and appropriate analytical methods because photo-interpretation methods (as those used here) cannot provide reliable information on quantitative plant properties. In addition, image processing and information retrieval methods would have to suit leaf size constraints, including finer pixel size and object-based analysis (*i.e.*, [64]).

5. Conclusions

Current practices of field gap evaluation in sugarcane plantations are highly demanding in terms of human labor and hence of very limited spatial intensity. For example, in this area of study, the rate was one segment of 30 m evaluated every 0.7 ha, which implies a length approximately equivalent to 0.45% of the total crop lines length. This sampling intensity is clearly insufficient to map gap percent and derived crop quality, which makes re-planting difficult to guide. Instead, our method, based on the processing of the digital mosaic of UAV images, estimates linear gap percentage with an RMSE of only 5.04 for a grid of 10 m $\times$ 10 m resolution, and derived Crop Planting Quality highly agreed with those derived from a photo-interpreted version of the currently used Stolf's method (Spearman's correlation coefficient 0.92). Furthermore, a map of canopy gaps is produced with high overall accuracy (97% estimated by cross-validation; 92.9% estimated by independent sample) at 23.5 cm resolution. Although some image processing improvements in image quality and processing can probably further reduce the error, the current methodology is ready for immediate operational application.

Previous results based on satellite imagery and hand-held spectroradiometry, together with the effectiveness of UAVs to image sugarcane crops at high resolution and the power of current processing methods as shown in this article, indicate the interest of replacing the conventional RGB imagery used in this study with multi-spectral imagery, to go beyond gap mapping into mapping plant status.

Acknowledgments: All UAV equipment, campaign costs and part of personnel costs (Inti Luna) were funded by Evolo, Nicaragua, a company of which Inti Luna is CEO and founder. We appreciate the help of the Evolo team formed by Fernando Luna, Roberto Luna and Fernando Tapia during the aerial campaign. We appreciate the support from the Erasmus Mundus Scholarship Program that made possible the Joint European Master in Environmental Studies carried out by Inti Luna, during which collaboration with Agustín Lobo started. We are grateful to the anonymous reviewers for their comments and recommendations that helped us improve this article. Finally, we would like to thank the international open source community for their contributions to software and code development present in R and QGIS.

Author Contributions: Inti Luna designed the study under the guidance of Agustín Lobo; Inti Luna coordinated the Evolo technical team to carry out the aerial campaign, Inti Luna processed the individual images into the mosaic; Agustín Lobo planned the statistical analysis and wrote the R functions; Inti Luna and Agustín Lobo wrote the manuscript.

Conflicts of Interest: The authors declare no conflict of interest.

Abbreviations

The following abbreviations are used in this manuscript:

UAV	Unmanned Aerial Vehicle
UAS	Unmanned Aerial System
RPAS	Remote Piloted Aerial Aircraft System
FAO	Food and Agricultural Organization of the United Nations
RS	Remote Sensing
RGB	Red-Green-Blue color composite
CCD	Charge-Coupled Device
QGIS	Quantum Geographic Information System
RMSE	Root Mean Square Error
LDA	Linear Discriminant Analysis
CLAHE	Contrast Limited Adaptive Histogram Equalization
RTK	Real Time Kinematic
SfM	Structure from Motion
CSM	Crop Surface Model

References

1. FAO. *Handbook of Sugar Beet*; Agribussines; FAO: Italy, Roma, 2009.
2. Macedo, I.C.; Seabra, J.E.A.; Silva, J.E.A.R. Green house gases emissions in the production and use of ethanol from sugarcane in Brazil: The 2005/2006 averages and a prediction for 2020. *Biomass Bioenergy* **2008**, *32*, 582–595. [CrossRef]
3. Yadav, R.L.; Solomon, S. Potential of developing sugarcane by-product based industries in India. *Sugar Tech* **2006**, *8*, 104–111. [CrossRef]
4. FAOSTAT. Available online: http://faostat3.fao.org/download/Q/QC/E (accessed on 10 February 2016).
5. CNPA. *Production Report for Harvest 2014–2015*; Comision Nacional Productores de Azucar: Managua, Nicaragua, 2015; p. 1.
6. INIDE. *Censo Nacional Agropecuario*; INIDE: Managua, Nicaragua, 2012.
7. Fischer, G.; Teixeira, E.; Tothne, E.; van Velthuizen, H. Land use dynamics and sugarcane production. In *Sugarcane Ethanol: Contribution to Climate Change Mitigation and the Environment*; Wageningen Academic Publisher: Wageningen, The Netherlands, 2008; pp. 29–62.
8. Martinelli, L.A.; Filoso, S. Expansion of sugarcane ethanol production in Brazil: Environmental and social challenges. *Ecol. Appl.* **2008**, *18*, 885–898. [CrossRef] [PubMed]
9. Goldemberg, J.; Coelho, S.T.; Guardabassi, P. The sustainability of ethanol production from sugarcane. *Energy Policy* **2008**, *36*, 2086–2097. [CrossRef]
10. Altieri, M.A. The ecological impacts of large-scale agrofuel monoculture production systems in the Americas. *Bull. Sci. Technol. Soc.* **2009**, *29*, 236–244. [CrossRef]
11. Foley, J.A.; Ramankutty, N.; Brauman, K.A.; Cassidy, E.S.; Gerber, J.S.; Johnston, M.; Mueller, N.D.; O'Connell, C.; Ray, D.K.; West, P.C.; *et al.* Solutions for a cultivated planet. *Nature* **2011**, *478*, 337–342. [CrossRef] [PubMed]
12. CNPA. *Production Report for Harvest 2015–2016. First Estimate*; Comisión Nacional Productores de Azúcar: Managua, Nicaragua, 2016; p. 1.
13. Santos, F.; Borém, A.; Caldas, C. *Sugarcane: Agricultural Production, Bioenergy and Ethanol*; Academic Press: Cambridge, MA, USA, 2015.
14. Gascho, G.J. Water-sugarcane relationships. *Sugar J.* **1985**, *48*, 11–17.
15. Raper, R.L. Agricultural traffic impacts on soil. *J. Terramech.* **2005**, *42*, 259–280. [CrossRef]
16. Paula, V.R.; Molin, J.P. Assessing damage caused by accidental vehicle traffic on sugarcane ratoon. *Appl. Eng. Agric.* **2013**, *29*, 161–169. [CrossRef]
17. Stolf, R. Methodology for gap evaluation on sugarcane lines. *STAB Piracicaba* **1986**, *4*, 12–20.
18. Alvares, C.A.; de Oliveira, C.F.; Valadão, F.T.; Molin, J.P.; Salvi, J.V.; Fortes, C. *Remote Sensing for Mapping Sugarcane Failures*; Congresso Brasileiro de Agricultura de Precisao: Piracicaba, Brazil, 2008.

19. Molin, J.P.; Veiga, J.P.S.; Cavalcante, D.S.C. *Measuring and Mapping Sugarcane Gaps*; University of São Paulo: São Paulo, Brazil, 2014.
20. Tenkorang, F.; Lowenberg-DeBoer, J. On-farm profitability of remote sensing in agriculture. *J. Terr. Obs.* **2008**, *1*, 6.
21. Atzberger, C. Advances in Remote Sensing of agriculture: Context description, existing operational monitoring systems and major information needs. *Remote Sens.* **2013**, *5*, 949–981. [CrossRef]
22. Thenkabail, P.S.; Lyon, J.G.; Huete, A. *Hyperspectral. Remote Sensing of Vegetation*; CRC Press: Boca Raton, FL, USA, 2011.
23. Mokhele, T.A.; Ahmed, F.B. Estimation of leaf nitrogen and silicon using hyperspectral remote sensing. *J. Appl. Remote Sens.* **2010**, *4*, 043560.
24. Honkavaara, E.; Saari, H.; Kaivosoja, J.; Pölönen, I.; Hakala, T.; Litkey, P.; Mäkynen, J.; Pesonen, L. Processing and assessment of spectrometric, stereoscopic imagery collected using a lightweight UAV spectral camera for precision agriculture. *Remote Sens.* **2013**, *5*, 5006–5039. [CrossRef]
25. Abdel-Rahman, E.M.; Ahmed, F.B. The application of remote sensing techniques to sugarcane (*Saccharum* spp. hybrid) production: A review of the literature. *Int. J. Remote Sens.* **2008**, *29*, 3753–3767. [CrossRef]
26. Tulip, J.R.; Wilkins, K. Application of spectral unmixing to trash level estimation in billet cane. In Proceedings of the 2005 Conference of the Australian Society of Sugar Cane Technologists; PK Editorial Services Pty Ltd.: Bundaberg, Australia, 2005; pp. 387–399.
27. Simões, M.; Dos, S.; Rocha, J.V.; Lamparelli, R.A.C. Spectral variables, growth analysis and yield of sugarcane. *Sci. Agric.* **2005**, *62*, 199–207. [CrossRef]
28. Miphokasap, P.; Honda, K.; Vaiphasa, C.; Souris, M.; Nagai, M. Estimating canopy nitrogen concentration in sugarcane using field imaging spectroscopy. *Remote Sens.* **2012**, *4*, 1651–1670. [CrossRef]
29. Schmidt, E.J.; Narciso, G.; Frost, P.; Gers, C. Application of remote sensing technology in the SA Sugar Industry–A review of recent research findings. In Proceedings of the 74th Annual Congress of the South African Sugar Technologists' Association, Durban, South Africa, 1–3 August 2000; Volume 74, pp. 192–201.
30. Zhang, C.; Kovacs, J.M. The application of small unmanned aerial systems for precision agriculture: A review. *Precis. Agric.* **2012**, *13*, 693–712. [CrossRef]
31. Rey, C.; Martín, M.P.; Lobo, A.; Luna, I.; Diago, M.P.; Millan, B.; Tardáguila, J. Multispectral imagery acquired from a UAV to assess the spatial variability of a Tempranillo vineyard. In *Precision Agriculture '13*; Stafford, J.V., Ed.; Wageningen Academic Publishers: Wageningen, The Netherlands, 2013; pp. 617–624.
32. Primicerio, J.; Di Gennaro, S.F.; Fiorillo, E.; Genesio, L.; Lugato, E.; Matese, A.; Vaccari, F.P. A flexible unmanned aerial vehicle for precision agriculture. *Precis. Agric.* **2012**, *13*, 517–523. [CrossRef]
33. Zarco-Tejada, P.J. A new era in remote sensing of crops with unmanned robots. *SPIE Newsroom* **2008**. [CrossRef]
34. INETER. Available online: http://servmet.ineter.gob.ni/Meteorologia/climadenicaragua.php (accessed on 8 February 2016).
35. INETER. *Taxonomia de Suelos de Nicaragua*; Publisher INETER: Managua, Nicaragua, 1975.
36. Quantum GIS Development Team. Quantum GIS Geographic Information System, Open Source Geospatial Foundation 2009. Available online: http://qgis.osgeo.org (accessed on 13 June 2016).
37. R Core Team. *R: A Language and Environment for Statistical Computing*; R Foundation for Statistical Computing: Vienna, Austria, 2012.
38. Keitt, T.H.; Bivand, R.; Pebesma, E.; Rowlingson, B. *Rgdal: Bindings for the Geospatial Data Abstraction Library*. R package version. 2012. Available online: https://cran.r-project.org/web/packages/rgdal/index.html (accessed on 13 June 2016).
39. Hijmans, R.J.; van Etten, J. Raster: Geographic Analysis and Modeling with Raster Data, R Package Version, 2012. Available online: https://cran.r-project.org/web/packages/raster/index.html (accessed on 13 June 2016).
40. Bivand, R.; Rundel, C. *Rgeos:* Interface to Geometry Engine-Open Source (GEOS), R Package Version, 2015. Available online: https://cran.r-project.org/web/packages/rgeos/index.html (accessed on 13 June 2016).
41. Venables, W.N.; Ripley, B.D. *Modern. Applied Statistics with S*, 4th ed.; Springer: New York, NY, USA, 2002.
42. Wickham, H. *Ggplot2: Elegant Graphics for Data Analysis*; Springer: New York, NY, USA, 2009.

43. Wickham, H. The split-apply-combine strategy for data analysis. *J. Statist. Softw.* **2011**, *40*, 136992. [CrossRef]
44. Richards, J.A.; Jia, X. *Remote Sensing Digital Image Analysis: An Introduction*, 4th ed.; Springer Verlag: Berlin, Germany; Heidelberg, Germany, 2005.
45. Congalton, R.G. A review of assessing the accuracy of classifications of remotely sensed data. *Remote Sens. Environ.* **1991**, *37*, 35–46. [CrossRef]
46. Lobo, A. Image segmentation and discriminant analysis for the identification of land cover units in ecology. *IEEE Trans. Geosci. Remote Sens.* **1997**, *35*, 1136–1145. [CrossRef]
47. Laliberte, A.S.; Goforth, M.A.; Steele, C.M.; Rango, A. Multispectral Remote Sensing from unmanned aircraft: Image processing workflows and applications for rangeland environments. *Remote Sens.* **2011**, *3*, 2529–2551. [CrossRef]
48. Zhou, Z.; Huang, J.; Wang, J.; Zhang, K.; Kuang, Z.; Zhong, S.; Song, X. Object-oriented classification of sugarcane using time-series middle-resolution Remote Sensing data based on adaboost. *PLoS ONE* **2015**, *10*, e0142069. [CrossRef] [PubMed]
49. Mountrakis, G.; Im, J.; Ogole, C. Support vector machines in remote sensing: A review. *ISPRS J. Photogramm. Remote Sens.* **2011**, *66*, 247–259. [CrossRef]
50. Gil, A.; Lobo, A.; Abadi, M.; Silva, L.; Calado, H. Mapping invasive woody plants in Azores Protected Areas by using very high-resolution multispectral imagery. *Eur. J. Remote Sens.* **2013**, *46*, 289–304. [CrossRef]
51. Zuiderveld, K. Contrast limited adaptive histogram equalization. In *Graphics Gems IV*; Heckbert, P.S., Ed.; Academic Press Professional, Inc.: San Diego, CA, USA, 1994; pp. 474–485.
52. Burkart, A.; Aasen, H.; Alonso, L.; Menz, G.; Bareth, G.; Rascher, U. Angular dependency of hyperspectral measurements over wheat characterized by a novel UAV based goniometer. *Remote Sens.* **2015**, *7*, 725–746. [CrossRef]
53. Peña-Barragán, J.M.; Kelly, M.; de-Castro, A.I.; López-Granados, F. Object-based approach for crop row characterization in uav images for site-specific weed management. In Proceedings of the 4th GEOBIA, Rio de Janeiro, Brazil, 7–9 May 2012; pp. 426–430.
54. Berni, J.A.J.; Zarco-Tejada, P.J.; Sepulcre-Cantó, G.; Fereres, E.; Villalobos, F. Mapping canopy conductance and CWSI in olive orchards using high resolution thermal remote sensing imagery. *Remote Sens. Environ.* **2009**, *113*, 2380–2388. [CrossRef]
55. Zarco-Tejada, P.J.; Guillén-Climent, M.L.; Hernández-Clemente, R.; Catalina, A.; González, M.R.; Martín, P. Estimating leaf carotenoid content in vineyards using high resolution hyperspectral imagery acquired from an unmanned aerial vehicle (UAV). *Agric. For. Meteorol.* **2013**, *171–172*, 281–294. [CrossRef]
56. Westoby, M.J.; Brasington, J.; Glasser, N.F.; Hambrey, M.J.; Reynolds, J.M. "Structure-from-Motion" photogrammetry: A low-cost, effective tool for geoscience applications. *Geomorphology* **2012**, *179*, 300–314. [CrossRef]
57. Mancini, F.; Dubbini, M.; Gattelli, M.; Stecchi, F.; Fabbri, S.; Gabbianelli, G. Using unmanned aerial vehicles (UAV) for high-resolution reconstruction of topography: The structure from motion approach on coastal environments. *Remote Sens.* **2013**, *5*, 6880–6898. [CrossRef]
58. Sullivan, D.; Brown, A. High accuracy autonomous image georeferencing using a GPS/Inertial-aided digital imaging system. In Proceedings of the 2002 National Technical Meeting of The Institute of Navigation, San Diego, CA, USA, 28–30 January 2002.
59. Jones, H.; Sirault, X. Scaling of thermal images at different spatial resolution: The mixed pixel problem. *Agronomy* **2014**, *4*, 380–396. [CrossRef]
60. Bellvert, J.; Zarco-Tejada, P.J.; Girona, J.; Fereres, E. Mapping crop water stress index in a "Pinot-noir" vineyard: Comparing ground measurements with thermal remote sensing imagery from an unmanned aerial vehicle. *Precis. Agric.* **2014**, *15*, 361–376. [CrossRef]
61. Zarco-Tejada, P.J.; Diaz-Varela, R.; Angileri, V.; Loudjani, P. Tree height quantification using very high resolution imagery acquired from an unmanned aerial vehicle (UAV) and automatic 3D photo-reconstruction methods. *Eur. J. Agron.* **2014**, *55*, 89–99. [CrossRef]
62. Bendig, J.; Willkomm, M.; Tilly, N.; Gnyp, M.L.; Bennertz, S.; Qiang, C.; Miao, Y.; Lenz-Wiedemann, V.I.S.; Bareth, G. Very high resolution crop surface models (CSMs) from UAV-based stereo images for rice growth monitoring in Northeast China. *Int. Arch. Photogramm. Remote Sens. Spat. Inf. Sci.* **2013**, *40*, 45–50. [CrossRef]

63. Geipel, J.; Link, J.; Claupein, W. Combined spectral and spatial modeling of corn yield based on aerial images and crop surface models acquired with an unmanned aircraft system. *Remote Sens.* **2014**, *6*, 10335–10355. [CrossRef]
64. Calderón, R.; Navas-Cortés, J.; Zarco-Tejada, P. Early detection and quantification of verticillium wilt in olive using hyperspectral and thermal imagery over large areas. *Remote Sens.* **2015**, *7*, 5584–5610. [CrossRef]